Forest Chemicals Review
www.forestchemicalsreview.com
ISSN: 1520-0191
September-October 2021 Page No. 242-249
Article History: Received: 22 July 2021 Revised: 16 August 2021 Accepted: 05 September 2021 Publication: 31 October 2021

$Ba_{0.7}Sr_{0.3}TiO_3$ Ceramic Fibers Prepared via Precursors Linear Self-Assembly Nonhydrolytic Sol-Gel Method

Feng Jiang[1], Yin Li [1], Feng Guo [1,*], Zhijun Yan[3], Jinlin Xu[3], Wentao Fang[3], Tao Jiang[3], Xiaolong Huang [1], Qian Wu[2], Jianmin Liu[2], Weihui Jiang[1, 2, *]

[1]Department of Material Science and Engineering, Jingdezhen Ceramic University, Jingdezhen 333000, China
[2]National Engineering Research Center for Domestic & Builing Ceramics, Jingdezhen Ceramic University, Jingdezhen 333000, China
[3]Jingdezhen Oceano Ceramic Co., Ltd, Jingdezhen 333000, China
*Corresponding Author.

Abstract:

$Ba_{0.7}Sr_{0.3}TiO_3$ fibers were prepared via precursor self-assembly non hydrolytic sol-gel (NHSG) method, using barium acetate, titanium tetrachloride and strontium acetate as barium source, titanium source and strontium source, anhydrous ethanol as oxygen donor and anhydrous ethylene glycol as solvent. It is discovered that NHSG method is beneficial for Ba–O–Ti and Sr–O–Ti bonds formation via heterogeneous condensation. Bimolecular association structure of chlorotitanium ethoxide generated from reaction of titanium tetrachloride and ethanol, which is beneficial for precursors' self-linear assembling. Linear colloids with excellent spinnability form in this process. The novel $Ba_{0.7}Sr_{0.3}TiO_3$ ceramic fibers will be widely used in electronic flexible products.

Keywords*: Ceramics, $Ba_{0.7}Sr_{0.3}TiO_3$, Fibers, Dielectrics, Piezoelectric.*

I. INTRODUCTION

As the most important electronic components, capacitors account for a large part of the electronic components [1]. Output value of global capacitor components has broken through billions of dollars (US).With the develop rapidly of the information industry, the requirements for the performance of capacitors are getting higher and higher [2].

For the requirements to multifunction, miniaturization and flexibility of electronic products, components of capacitor should be flexibility, large capacity and miniaturization [3]. $Ba_{0.7}Sr_{0.3}TiO_3$ ceramic fiber has broad application prospects in embedded packaging components and high-power

Forest Chemicals Review
www.forestchemicalsreview.com
ISSN: 1520-0191
September-October 2021 Page No. 242-249
Article History: Received: 22 July 2021 Revised: 16 August 2021 Accepted: 05 September 2021 Publication: 31 October 2021

capacitors due to high energy storage density, high flexibility and dielectric constant [4-5]. Recent contributions have devoted to relative topics [6-8]. Pan [6] fabricated BST ($Ba_xSr_{1-x}TiO_3$)/ PVDF (polyvinylidene fluoride) fiber composites via near-field electrospinning (NFES) method, in which BST ceramic powders were mixed with PVDF to prepare piezoelectric fiber composites. Vigneshwaran [7] and He [8] investigated the effect of calcined time and temperature on structure and properties of $Ba_xSr_{(1-x)}TiO_3$ ceramics. Our team has developed a novel precursors linear self-assembly nonhydrolic sol-gel method [9]. In this work, the method is utilized to prepare novel $Ba_{0.7}Sr_{0.3}TiO_3$ ceramic fibers.

II. MATERIALS AND METHODS

2.1. Samples Preparation

Titanium tetrachloride (AR, $TiCl_4$, Shanghai), anhydrous barium acetate (AR, Ba $(OOCCH_3)_2$, Shanghai), anhydrous strontium acetate (AR, Sr $(OOCCH_3)_2$, Shanghai), glycol (AR, $(CH_2OH)_2$, Shanghai) and absolute ethanol (AR, EtOH, Shanghai) were selected as the raw material.

In accordance with the nominal composition of $Ba_{0.7}Sr_{0.3}TiO_3$ (the relative molar ratio of $Ba(OOCCH_3)_2$: $Sr(OOCCH_3)_2$: $TiCl_4$ = 0.7 : 0.3 : 1), add 4.1mL $TiCl_4$ slowly (about 10 mL/min) through a pipette in glove box into a 5.5mL anhydrous EtOH Erlenmeyer flask (100mL). After stirring for 6h, a transparent bright yellow $TiCl_4$-EtOH solution forms. After that, 17mL glycol is added to solution and stirring for 30 min. Then, 6.670g Ba $(OOCCH_3)_2$ and 2.403g Sr $(OOCCH_3)_2$ are added into the solution. And then, the solution is fluxed and agitated at 80°C for 2h and further aged at 60°C without stirring for 48h, obtaining spinnable sol with the viscosity of about 50Pa·S. The spinnable sol is fiber-formed by drawing with a glass rod at the speed of 0.5m/s. After fiber-forming, $Ba_{0.7}Sr_{0.3}TiO_3$ wet gel fibers are obtained, and they are dried at 80°C for 4h. Xerogels fibers were finally calcined at 700°C for 0.5 h to form the final fibers.

2.2 Characterization

Under the conditions of 40kV and 30mA, the phase of the sample was determined by X-ray diffractometer (XRD, Bruker) radiation using CuKα (λ=1.5405Å). Samples diffractograms were recorded in the 2θ range of 10-70° in steps of 0.02° with the count time of 0.2s (5s for XRD structural refinement). Morphology of sol is characterized by transmission electron microscopy (TEM, JEOL). The microstructure of fibers is observed by field-emission scanning electronmicroscopy (FE-SEM, JEOL). The thermolysis process of xerogels is tested by thermogravimetric and differential thermal analysis analysis (DTA-TG, NETZSCH) (Heating rate: 10℃/min, test temperature range: room temperature-900°C, test atmosphere: air atmosphere). The bonds of the samples are tested in the range of 400-4000 cm^{-1} by Fourier transform infrared spectroscopy (FT-IR, Thermo).

Forest Chemicals Review
www.forestchemicalsreview.com
ISSN: 1520-0191
September-October 2021 Page No. 242-249
Article History: Received: 22 July 2021 Revised: 16 August 2021 Accepted: 05 September 2021 Publication: 31 October 2021

III. RESULTS AND DISCUSSION

Fig. 1(a) displays the DTA-TG patterns of fibers xerogel. Fig. 1(b) presents corresponding XRD patterns.

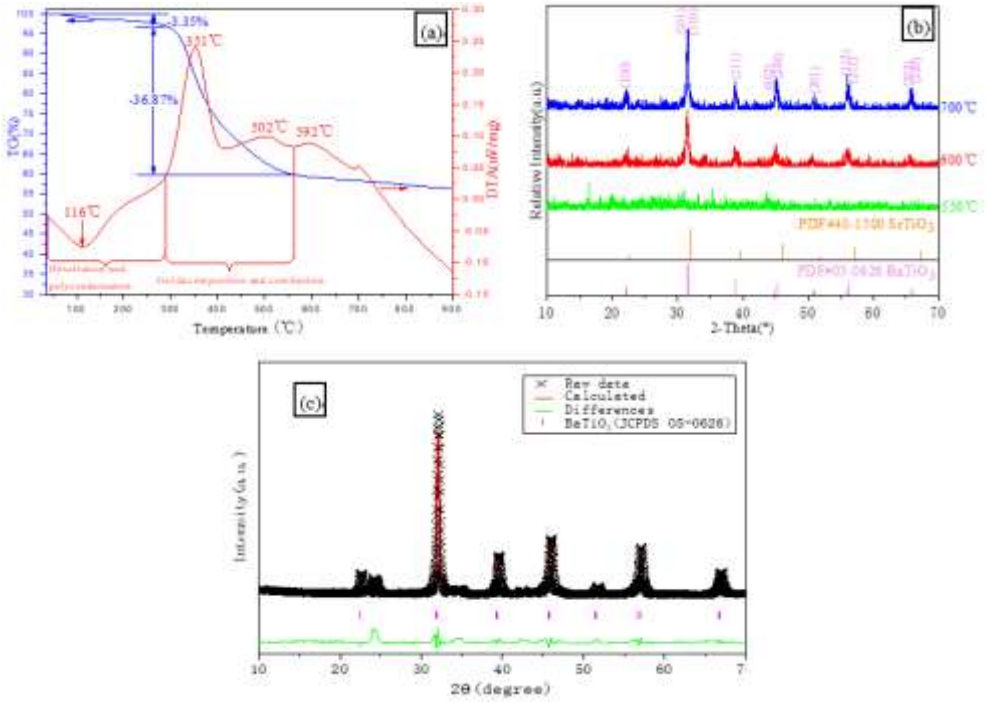

Fig 1: DTA-TG curves of xerogel (a), XRD patterns of samples prepared at different temperatures (b) and refinement of XRD pattern (c)

DTA curve of $Ba_{0.7}Sr_{0.3}TiO_3$ ceramic xerogel presents an obvious endothermic peak located at 116°C, which corresponds to 3.35wt.% weight loss from the corresponding temperature range (room temperature~270°C) on the TG curve. This is due to the further solvation and condensation of xerogels. The second exothermic peak cauterized at 351°C, which is due to the decomposition of the xerogel. The third exothermic peak locates at 502°C, and it is caused by the combustion of the xerogel. The fourth exothermic peak is concentrated at 592°C. Combined with the samples calcined at 500°C and 600°C without any obvious weight loss and phase transformation, and the exothermic peak at 592°C is confirmed to the crystallization of $BaTiO_3$. The sample crystallinity calcined at 700°C is higher than that of sample at 600°C. Compared with the standard diffraction card of $BaTiO_3$ (JCPDS Card No. 05-0626), all diffraction peaks move slightly to a higher angle. In addition, rietveld refinement is used to analyze the cell parameters of barium strontium titanate and Fig.1(c) shows the refinement results. The cell

Forest Chemicals Review
www.forestchemicalsreview.com
ISSN: 1520-0191
September-October 2021 Page No. 242-249
Article History: Received: 22 July 2021 Revised: 16 August 2021 Accepted: 05 September 2021 Publication: 31 October 2021

parameters before and after refinement are a=b=c=3.985 (Vol = 63.283) and 3.961 (Vol = 62.159), respectively. These results indicate Sr^{2+} has been doped into the crystal lattice of barium titanate.

The TEM of the sol is shown as Fig. 2 (a) and (b). As can be seen from Fig. 2(a), there are clear needle-like or rod-like colloids. The diameters of the needle-like or rod-like colloids are about 0.1 - 0.25μm, and the aspect ratios of $Ba_{0.7}Sr_{0.3}TiO_3$ ceramic fibers are larger than 10. The higher magnification shown as Fig. 2(b) shows the linear sol particle is in solid rod state. These results confirm that the precursors can linearly self-assemble to needle-like or rod-like colloids which are widely regarded as the premise of fiber forming by sol-gel method. Although the surface of colloids is not very smooth and there are also granular colloids with blurred outline. Fig. 2(c) (d) is FE-SEM images of $Ba_{0.7}Sr_{0.3}TiO_3$ ceramic fibers, it can be seen that it is a typical SEM micrograph of the fiber. The mean diameter of $Ba_{0.7}Sr_{0.3}TiO_3$ ceramic fibers is determined as about 2-2.5μm. The aspect ratios of $Ba_{0.7}Sr_{0.3}TiO_3$ ceramic fibers are larger than 10. Although there are obvious a few spotted defects on both the surface and the cross-section of the fibers, the fibers are overall smooth in surface and in solid state in cross-section.

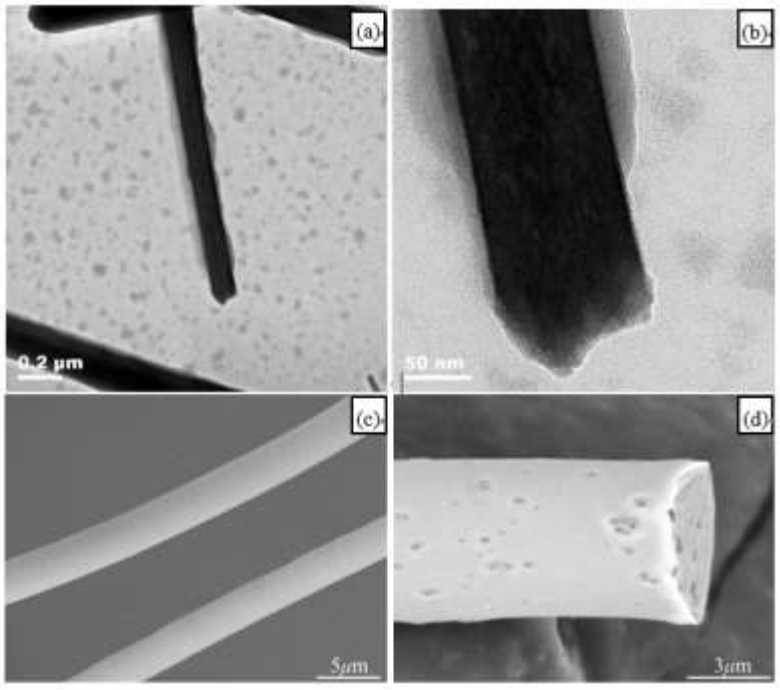

Fig 2: TEM graphs of sol (a) (b) and FE-SEM graphs of fibers (c) (d)

Fig.3 shows the EDS-mapping of fibers. From Fig.3 can be seen, the fibers show considerable homogeneity and highly consistent in composition with the nominal composition.

Forest Chemicals Review
www.forestchemicalsreview.com
ISSN: 1520-0191
September-October 2021 Page No. 242-249
Article History: Received: 22 July 2021 Revised: 16 August 2021 Accepted: 05 September 2021 Publication: 31 October 2021

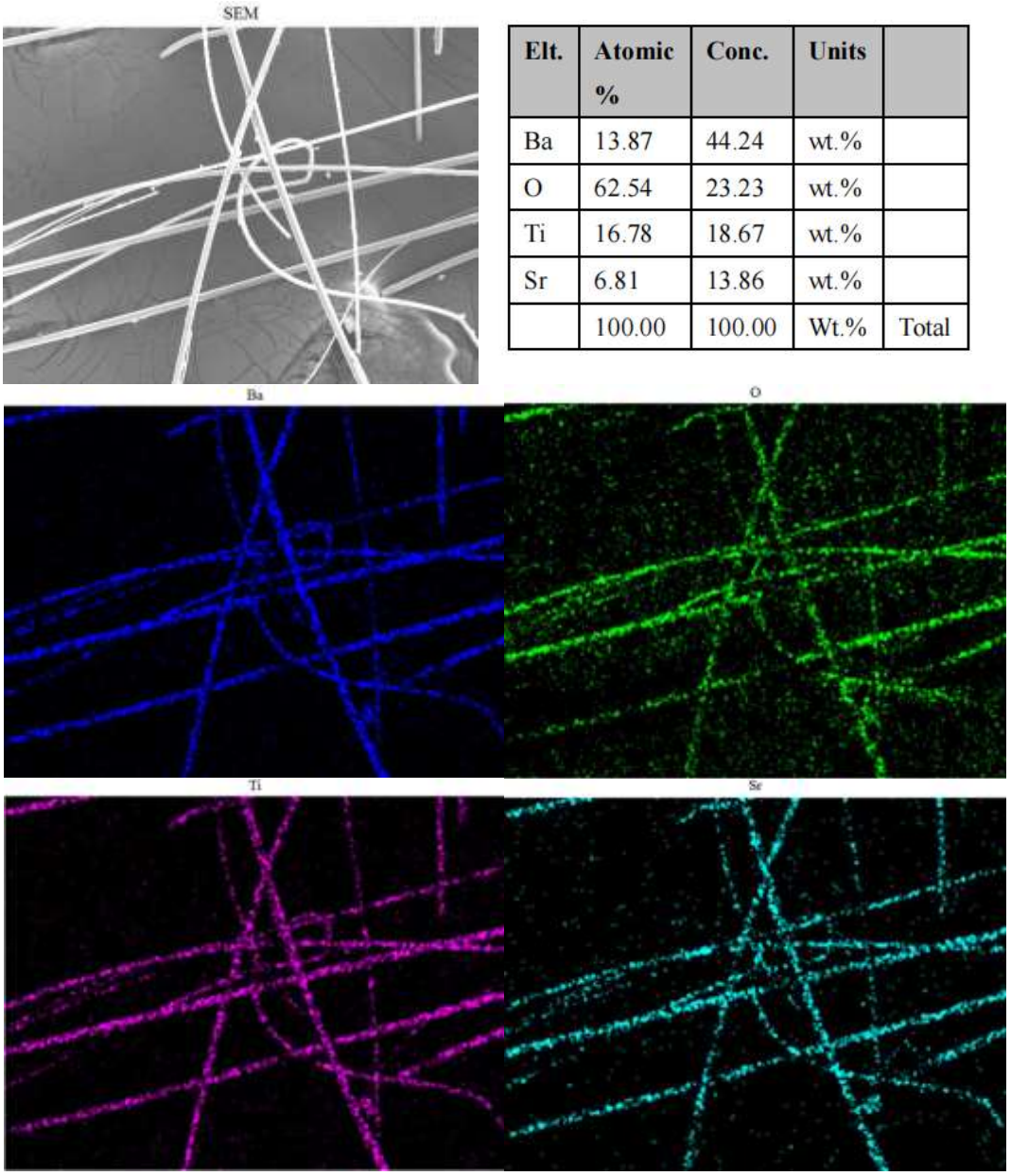

Elt.	Atomic %	Conc.	Units	
Ba	13.87	44.24	wt.%	
O	62.54	23.23	wt.%	
Ti	16.78	18.67	wt.%	
Sr	6.81	13.86	wt.%	
	100.00	100.00	Wt.%	Total

Fig 3: EDS-mapping of fibers

In order to study the synthesis mechanism of $Ba_{0.7}Sr_{0.3}TiO_3$ fibers, particularly the formation mechanism of linear colloids. FI-IFR spectra analysis was carried out on the samples prepared in different periods in the NHSG process, and the analysis is shown in Fig. 4(a). v(C-O) H bonds disappear in sample (II) EtOH + $TiCl_4$ compared with sample (I) EtOH and (II) EtOH + $TiCl_4$ [10]. In contrast, Ti (O-C) and Ti-Cl bonds appear at 795 cm^{-1} and 889 cm^{-1}[11]. These certificate the reaction between

Forest Chemicals Review
www.forestchemicalsreview.com
ISSN: 1520-0191
September-October 2021 Page No. 242-249
Article History: Received: 22 July 2021 Revised: 16 August 2021 Accepted: 05 September 2021 Publication: 31 October 2021

anhydrous EtOH and titanium tetrachloride, which is shown as equation (1) [12]. Chlorotitanium ethoxide ($TiCl_2(OEt)_2$) is the reaction intermediate and has the bimolecular association structure as shown in the left side of Fig. 4 (b) for meeting the hexa-coordination demand of Ti. At the same time, owing to the reaction activities differences of EtO and Cl groups, the CH_3COO prefer to reacts with EtO group for deacetylation reaction. The formation of Ba-O-Ti bond and Sr-O-Ti bond at 1418cm^{-1} [13] and 1340cm^{-1} [14]. Consequently, chlorotitanium ethoxide, Ba $(OOCCH_3)_2$ and $Sr(OOCCH_3)_2$ ultimately assemble to form linear colloids shown as Fig.2(a) and (b). Fig. 4(b) shows the mechanism for precursors linear-assembling process.

$$2EtOH + TiCl_4 \rightarrow TiCl_2(OEt)_2 + 2HCl \quad (1)$$

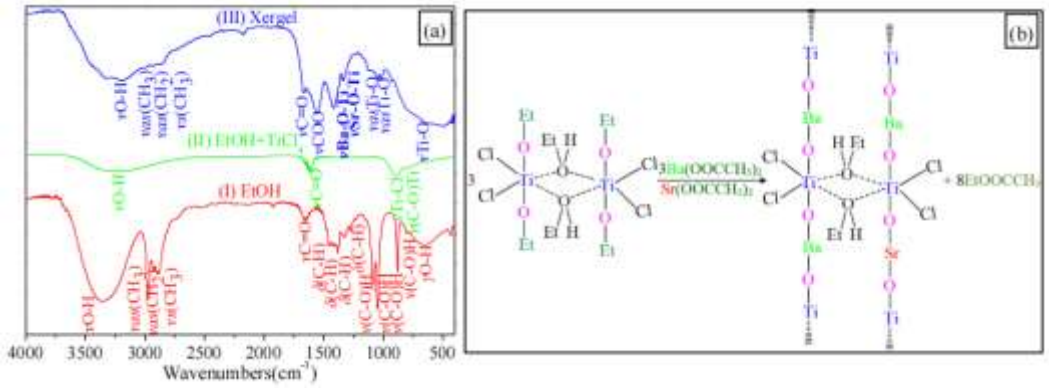

Fig 4: FT-IR spectra of samples (a) and linear-assembly mechanism of precursors (b)

IV. CONCLUSION

Linear self- assembly NHSG method is innovatively applied to prepare novel $Ba_{0.7}Sr_{0.3}TiO_3$ ceramic fibers. The average diameter of $Ba_{0.7}Sr_{0.3}TiO_3$ ceramic fibers are about 2-2.5μm, The aspect ratio of $Ba_{0.7}Sr_{0.3}TiO_3$ fibers is more than 10, smooth of surface and solid in cross-section structure with a few spotted defects. Bimolecular association structure of chlorotitanium ethoxide which generated from the reaction of titanium tetrachloride and anhydrous ethanol, which promotes the precursors self-linear-assembly. The precursor self-assembly of non hydrolytic sol-gel method is a new method to prepare ceramic fibers, due to its advantages of excellent molecular economy, high target elements content in the precursor fibers, and not easy to pulverize, fracture and crack in the subsequent ceramic crystallization process.

Forest Chemicals Review
www.forestchemicalsreview.com
ISSN: 1520-0191
September-October 2021 Page No. 242-249
Article History: Received: 22 July 2021 Revised: 16 August 2021 Accepted: 05 September 2021 Publication: 31 October 2021

ACKNOWLEDGMENTS

This work should express acknowledgments to National Natural Science Foundation of China [No. 51962014, 52072162]; Natural Science Foundation of Jiangxi Province [No. 20192BBEL50022, 20202ACBL214006, 20202ACBL214008, 20202BABL214013, 2020ZDI03004, 20202BABL214013, 20212BBE53048]; the Open fund project of Key Laboratory of Inorganic Coating Materials, Chinese Academy of Science (No. ICM-202001); Science Foundation of the Department of Education of Jiangxi Province (No. GJJ201345, GJJ201324); the science and technology plan project of Jingdezhen (No. 2020GYZD013-09, 2020GYZD013-14, 2021ZDGG001).

REFERENCES

[1] Fedorovskaya EO, Bulusheva LG, Kurenya AG, Asanov IP, Rudina NA, Funtov KO, Lyubutin LS, Okotrub AV (2014) Supercapacitor performance of vertically aligned multiwall carbon nanotubes produced by aerosol-assisted CCVD method. Electrochimica Acta 139:165-172

[2] Asrar A (2020) Screen-printed activated carbon/silver nanocomposite electrode material for a high performance supercapacitor. Materials Letters 273:127933

[3] Yuan H, Wang G, Zhao YX, Liu Y, Wu Y, Zhang YG (2020) A stretchable, asymmetric, coaxial fiber-shaped supercapacitor for wearable electronics. Nano Research 13:1686-1692.

[4] Kim JK, Kim SS, Kim WJ, Ha TG, Kim IS, Song JS, Guo R, Bhalla AS (2006) Improved ferroelectric properties of Cr-doped $Ba_{0.7}Sr_{0.3}TiO_3$ thin films prepared by wet chemical deposition. Materials Letters 60:2322-2325

[5] Guo HL (2004) The effect of sintering on the properties of $Ba_{0.7}Sr_{0.3}TiO_3$ ferroelectric films produced by electrophoretic deposition. Materials Letters 58:1387-1391

[6] Pan CT, Wang SY, Yen CK, Kumar A, Kuo SW, Zheng JL, Wen ZH, Singh R, Singh SP, Tahir KM, Kumar RC, Dai XF, Chandra AK, Wei DQ, Shiue YL, Chang WH (2020) Polyvinylidene fluoride-added ceramic powder composite near-field electrospinned piezoelectric fiber-based low-frequency dynamic sensors. ACS Omega 28:17090-17101

[7] Vigneshwaran B, Kuppusami P, Ajithkumar S, Sreemoolanadhan H (2020) Study of low temperature-dependent structural, dielectric, and ferroelectric properties of $Ba_xSr_{(1-x)}TiO_3$ (x=0.5, 0.6, 0.7) ceramics. Journal of Materials Science: Mateirals in Electronics 31:10446-10459

[8] He HF, Cai W, Gao RL, Chen G, Deng XL, Wang ZH, Fu CL (2019) Effects of sintering time on microstructure and electric properties of $Ba_{0.7}Sr_{0.3}TiO_3$ ceramics, Ferroelectrics 551:5-16

[9] Feng G, Jiang F, Jiang WH, Liu JM, Zhang Q, Wu Q, Hu Q, Miao LF, Liang J (2019) Low-temperature preparation of novel stabilized aluminum titanate ceramic fibers via nonhydrolytic sol-gel method through linear self-assembly of precursors, Ceramics International 45:18704-18709

[10] Zhu YF, Zhang L, Gao C, Cao LL (2000) The synthesis of nanosized TiO_2 powder using a sol-gel method with $TiCl_4$ as a precursor. Journal of Materials Science 35:4049-4054

[11] Bradley DC, R. C. Methrotra, D. P. Gaul, Metal Alkoxides, New York: Academic Press 92:975-975

Forest Chemicals Review
www.forestchemicalsreview.com
ISSN: 1520-0191
September-October 2021 Page No. 242-249
Article History: Received: 22 July 2021 Revised: 16 August 2021 Accepted: 05 September 2021 Publication: 31 October 2021

[12] Albury AMM, Jennings MP (2013) $TiCl_4$ mediated preparation of (E)-non-conjugated homoallylic alcohols with α-substituted allylsilanes. Tetrahedron Letters 54:4487-4490

[13] Kamalasanan MN (1994) Structural and microstructural evolution of $BaTiO_3$ thin films deposited by the sol-gel process. Journal of Applied Physics 76:4603-4609

[14] Chen WK Cheng CM, Huang JY, Hsieh WF, Tseng TY (2000) Study of linear and nonlinear optical properties of distorted Ti–O_6 perovskite structure in $Ba_xSr_{1-x}TiO_3$. Journal of Physics and Chemistry of Solids 61:969-977